THE MODAL SPECTRUM OF FERRITE-LOADED STRIPLINES

by

Donald M. Bolle
Division of Engineering
BROWN UNIVERSITY
Providence, Rhode Island 02912

Abstract

This paper presents the latest results of a theoretical investigation into the full modal spectrum of those ferrite-loaded planar waveguiding structures which represent the device geometries employed in broad-band stripline isolators and circulators.

Introduction

The promise of broad-band isolators and circulators in the S through K band, using the edge-guided or peripheral modes, having performance characteristics throughout the band which compare with or exceed those obtained from more conventional components, has not been realized despite rather extensive developmental work in the U.S., Europe and Japan.(1-8)

It has been evident that an inadequate theoretical basis existed against which to correlate experimental data and with which sufficient insight into the device operation could be developed.

Our earlier studies (9-10) investigated the edge-guided or peripheral mode and established the bandwidth to be expected if device operation was restricted to the utilization of such modes. In addition, we investigated the relationship between the surface modes on appropriate canonical structures and the edge-guided mode. It was concluded that the edge-guided mode is a perturbed surface mode, and exists only in that range of frequencies where the effective permeability $[1 + \chi - \kappa^2/(1 + \chi)]$ is negative. Furthermore, the mode adheres rather 'tightly' to the edge of the stripline and is highly dispersive.

From experimental work by deSantis (5,6) and Rosenbaum (7) it became evident that devices which were presumed to depend on the edge-guided mode in fact continued to operate beyond those frequencies where the edge-guided mode could exist. The earlier work concentrated on the geometry shown in Figure 1(a), i.e., the ferrite dielectric interface between two parallel conducting plates supporting the surface mode, and Figure 1(c), the ferrite-dielectric interface with the conducting half-plane which supports the edge-guided mode. This latter structure is the canonical geometry for the symmetric stripline [Figure 1(b)], where we assume no interaction between the stripline edges thus leading us to the semi-infinite plate representation for the central conductor. Figure 2 shows presentative results obtained for the three lowest order unidirectional surface modes of geometry 1(a), and also the corresponding unidirectional edge-guided modes for geometry 1(c). No other modes are to be found for these restricted model structures.

To investigate the broad-band behavior of these planar devices, the analysis had to be extended to geometries with finite width which then represented more closely the actual device structures. We therefore considered the geometries of Figure 3. Our ultimate objective is the shielded microstrip structure shown in Figure 3(c), where we must include both ferrite and conductor losses. However, we restrict ourselves first to the stripline of Figure 3(b), which leads to the canonical structure shown in 3(a). The latter structure should related to the more realistic model of 3(b) in the same manner that the results for the geometry in Figure 1(a) related to the results for Figure 1(c). Qualitatively, they compare readily though qualitatively there exist significant departures.

The geometry of Figure 3(a) has been investigated by Courtois [Ref. (3)] at an earlier date. It was decided to re-examine this structure in view of the fact that deSantis observed that continuous device operation can be, and is, obtained as one increases the frequency starting from $f = \sqrt{f_o(f_o + f_n)}$, $f_o = \gamma H_{d.c.}$ and $f_m = \gamma 4\pi M_s$, where the effective permeability first becomes negative and where we obtain the onset of the edge-guided mode. Courtois in his results appears to show that a definite band gap exists between the edge-guided ['magnetostatique'] mode, and the "waveguide" ['dynamique'] modes. As mentioned, deSantis has not observed such a stop band.

Results and Discussion

Figure 4 and 5 illustrate the nature of our results obtained for the lowest order TE mode (n=0) and for a typical ferrite material employed in the canonical stripline geometry of Figure 3(a). These results differ significantly from those obtained by Courtois. First, the waveguide modes are shown to overlap with the edge-guided mode regime. Secondly, the 'volume' modes which occur below the frequency band where the effective permeability is negative show a much more gradual cut-off than was obtained in Courtois' study. (Note that for this geometry, the modes are not unidirectional and the ω-β diagram is symmetric about β=0.)

It is interesting to observe the nature of the transverse field distribution for these lowest order modes ($\partial/\partial y = 0$). Below the surface mode band ($\mu_{effec} < 0$) we observe volume modes which do not exist in the isotropic case and thus, are due entirely to the particular anisotropic nature of the ferrite; secondly, the surface mode displays the well-known adherence to the ferrite-dielectric interface, which results from the same field displacement effect observed in the transversely magnetized ferrite slab loaded rectangular waveguided and again, does not occur for a dielectric/free space interface, thirdly, the 'waveguide' modes which, for sufficiently high frequencies, show the same behavior and field distribution as would be the case for an isotropic dielectric slab, while in the region where we have negative effective μ and transverse hyperbolic functional dependence exists we see a modified distribution with, by far, the greater field intensity at the opposite face of the ferrite slab to the one which supports the surface mode.

In Figure 4, we also show the higher order 'waveguide' modes and the transverse distribution of the electric field intensity for these modes only. The broken line curves show the lowest two modes for the corresponding isotropic case. It is evident that the bandwidth of the surface mode is limited. In this particular case, for a material with $4\pi M_s$ = 1760 Gauss the maximum useful band extends from 1.8 GHz to about 2.8 GHz, i.e., about 50%. It appears, therefore, that devices which exhibited measured bandwidth of two to three octaves, say 2 to 8 GHz, may in fact have been using the waveguide mode in that region where the transverse field distribution is akin to that of a surface mode.

We observe that for a slab width of 5 mm. the electric field intensity at x = b is approximately three times that at x = 0. Increasing the width of the ferrite slab to 10 mm. enhances the quasi-surface nature of the lowest order (zero cut-off) 'waveguide' mode. Figure 5 shows the dispersion characteristics for this wider case, while Figure 6 shows some representative transverse electric field intensity distributions. The horizontal broken lines indicate the limits of the region where the effective permeability is negative, i.e., $1.8 \leq F \leq 5.5$ GHz. The dash-dot curves indicate the limits of the region where the functional behavior of the fields changes from exponential to trigonometric form, i.e., in the region between these curve the transverse behavior of the field components is hyperbolic.

The lighter solid line gives the results for the case where the ferrite magnetization has been reduced to zero, thus yielding the corresponding results for the isotropic case. Only the two lowest order modes are shown. Figure 6 gives the transverse fields distribution at points A through D for this case, and allows comparison with the perturbed structure obtained for the anisotropic ferrite case. The transverse field distributions obtained for points G through K indicate the substantial departure from the isotropic distributions and show a pronounced quasi-surface wave character with ratios of the electric field strengths in excess of ten to one at the opposing faces of the ferrite slab over a frequency range from about 2 to 8 GHz. In fact, we do not begin to approach the symmetric distribution characteristic of the isotropic 'waveguide' modal form until the neighborhood of 10 GHz is reached and we are well into the region where the field expressions becomes of trigonometric form. We also show the next higher order isotropic and anisotropic modes and examples of their transverse field behavior at points M and N. We again show the two lowest order volume modes and their transverse distributions at points E and F. Particularly pertinent is the fact that the waveguide mode approached the asymptote $\omega=\beta c_o$ much more rapidly than is the case for the isotropic mode as we reduce the frequency. The surface mode approached the limit $f = [f_o(f_o+ f_m)]^{1/2}$ and is cut-off before merging with the c_o asymptote.

Computational difficulty prevents the tracing of the zero order 'waveguide' mode along the c_o asymptote in the region where the surface mode approaches and the volume modes join this asymptote.

Conclusions

It is apparent that the quasi-surface mode behavior and structure of the basic stripline (waveguide) mode may have led to its being confused with the surface or 'edge-guided' mode. We have seen that the maximum bandwidth of the edge-guided or surface mode does not begin to approach the experimentally observed bandwidth of devices which, in fact, must operate by using the quasi-surface modal structure assumed by the basic stripline mode. For low loss broad-band operation, it becomes important then that not only do we not use the surface mode, but we must suppress it, since it is guided on the face opposite to the one which supports the broad-band mode. Any energy fed into the surface mode will only increase the isolator forward loss and substantially impair isolation in the reverse direction. For the parameters selected here this means that the effective bandwidth is reduced by about 1 GHz and is restricted to the approximate range of 3 to 8 GHz.

Current efforts are directed towards introducing ferrite loss into our computations and to extending our treatment to the more representative geometry of Figure 3(b).

Acknowledgements

This research was supported through NSF Grant ENG 74-14187 and ONR Contract N000 14-75-C-0750. The help of Mr. Salvador Talisa with some of the computational work is gratefully acknowledged.

References

[1] M. E. Hines, *Reciprocal and Nonreciprocal Modes of the Propagation in Ferrite Stripline and Microstrip Devices*, IEEE Trans. MTT, Vo. MTT-19. No. 5., pp. 442-451, May 1971.

[2] L. Courtois, et al., *Propagation dans une lame de ferrite aimantee: Application a de nouveaux despositifs non-reciproques a large bande*, Cables et Telecommunications, No. 4, pp. 417-435, October 1973.

[3] L. Courtois, *Propagation oblique des ondes electromagnetiques dans une lame de ferrite aimantee parallelement a ses faces*, Electron. Fisc. Apli., Vol. 16, No. 2., pp. 286-294, 1973.

[4] L. Courtois, et al., *A New Edge Mode Isolator in the u.h.f. Range*, 1974 IEEE International Microwave Symposium Digest, Atlanta, June 12-14, 1974.

[5] P. deSantis, *Edge Guided Modes in Ferrite Microstrips With Curved Edges*, Applied Physics, Vol. 4, No. 2., pp. 167-174, August 1974.

[6] G. Cortussi and P. deSantis, *Edge-guided Waves in Lossy Ferrite Microstrip*, Proc. Euro. Micro. Conf., Vol. 2., pp. B9-1, September 1973.

[7] T. S. Wu and F. J. Rosenbaum, *Wide Band Opera-*

tions of Microstrip Circulators, IEEE Trans. MTT-22, pp. 249-285, October 1974.

[8] R. Araki, et al., *A New Type Isolator Using the Edge-guided Mode*, IEEE Trans. MTT, Vol. MTT-23, No. 3, pp. 321, March 1975.

[9] D. M. Bolle, *The Edge-guided Mode on Ferrite Loaded Stripline*, 1976 IEEE MTT International Microwave Symposium Digest, pp. 257-259, June 1976.

[10] D. M. Bolle, *The Peripheral or Edge-guided Modes on the Inhomogeneously and Homogeneously Ferrite-Loaded Stripline*, The 6th European Microwave Conference Digest, pp. 560-564, September 1976.

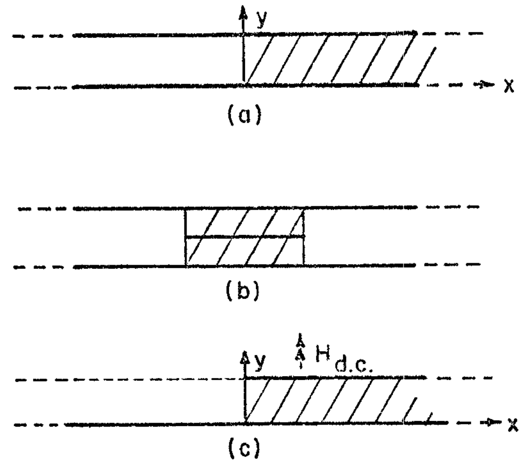

FIGURE 1

Stripline Geometries a) surface mode structure, b) ferrite loaded stripline geometry, c) canonical stripline geometry.

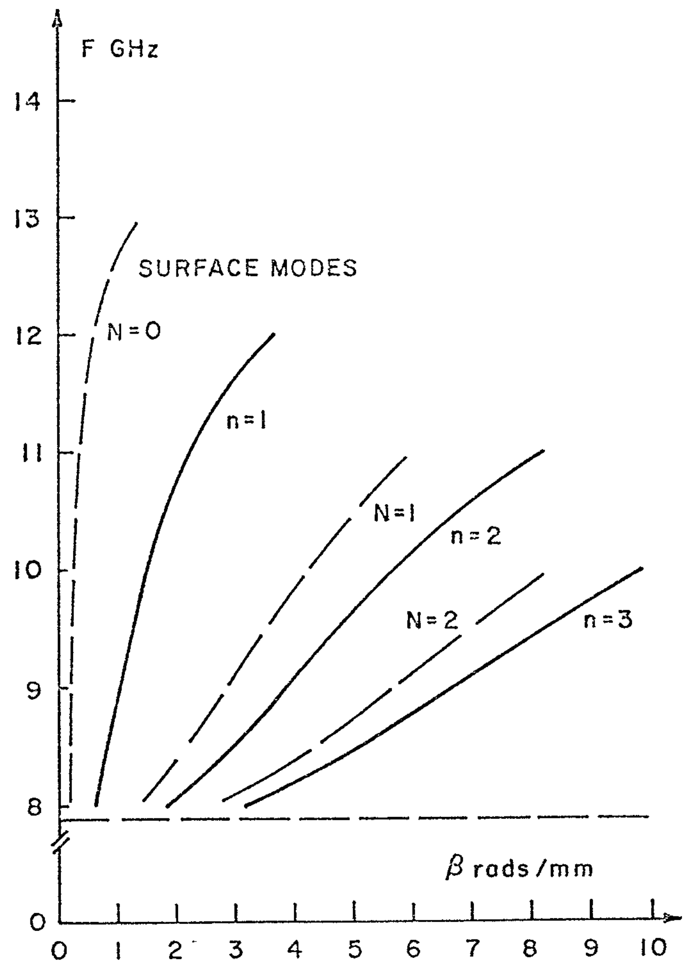

FIGURE 2

The Surface and Edge-Guided Modes Compared, Dispersion Characteristics, $4\pi M_s$ = 4250. G., $H_{D.C.}$ = 1400. Ø., ε_F = 12.3, ε_D = 1.0, D = .6mm.

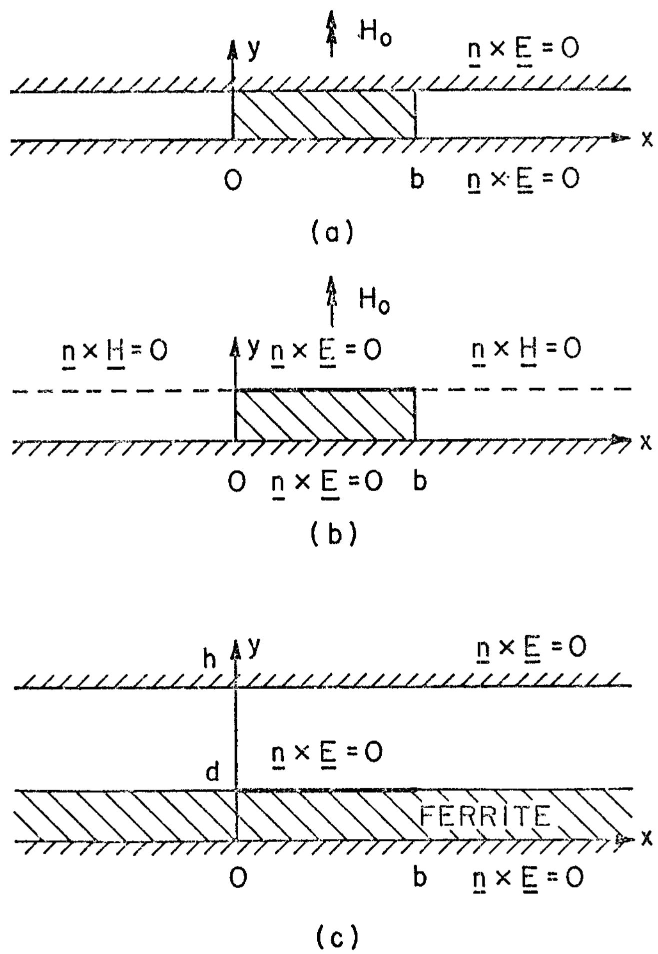

FIGURE 3

(a) Canonical ferrite-loaded stripline structure,
(b) the symmetric stripline geometry
(c) shielded microstripline.

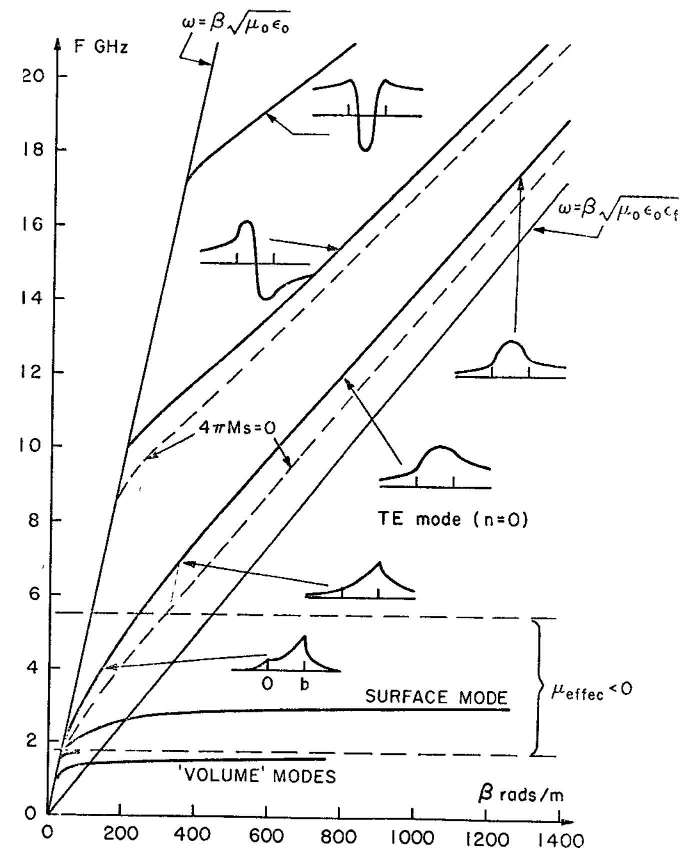

FIGURE 4

Dispersion characteristics and transverse field distributions for the lowest order modes ($\partial/\partial y = 0$) for the canonical ferrite loaded stripline structure of Fig. 12(a). [$4\pi M_s$ = 1760 G., H_o = 200ϕ, ϵ_f = 15., ϵ_d = 1.0, b = 5mm.] Dotted lines give the characteristics for the corresponding isotropic case, $\chi = \kappa = 0$.

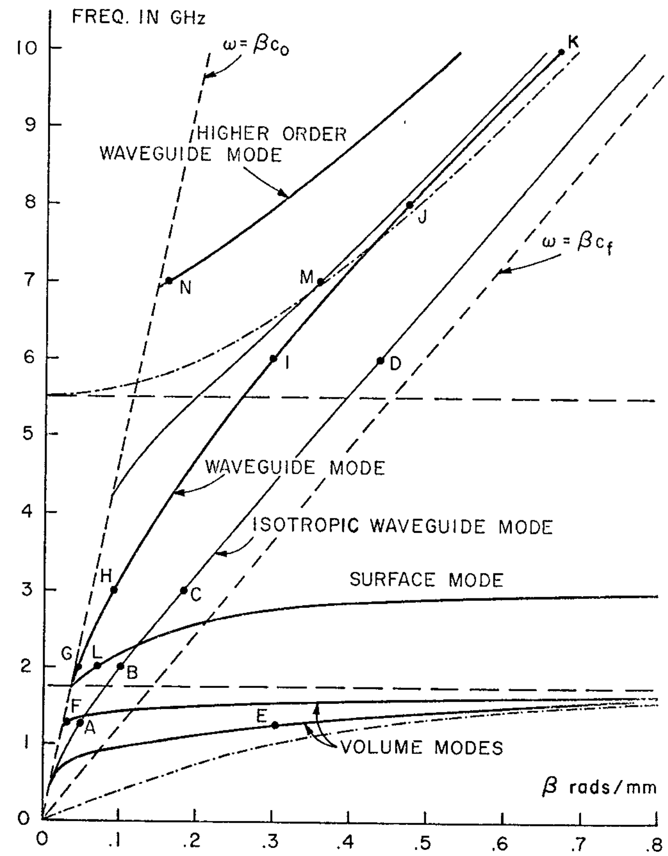

FIGURE 5

Results corresponding to those for Figure 4 for increase in width b to 10 mm.

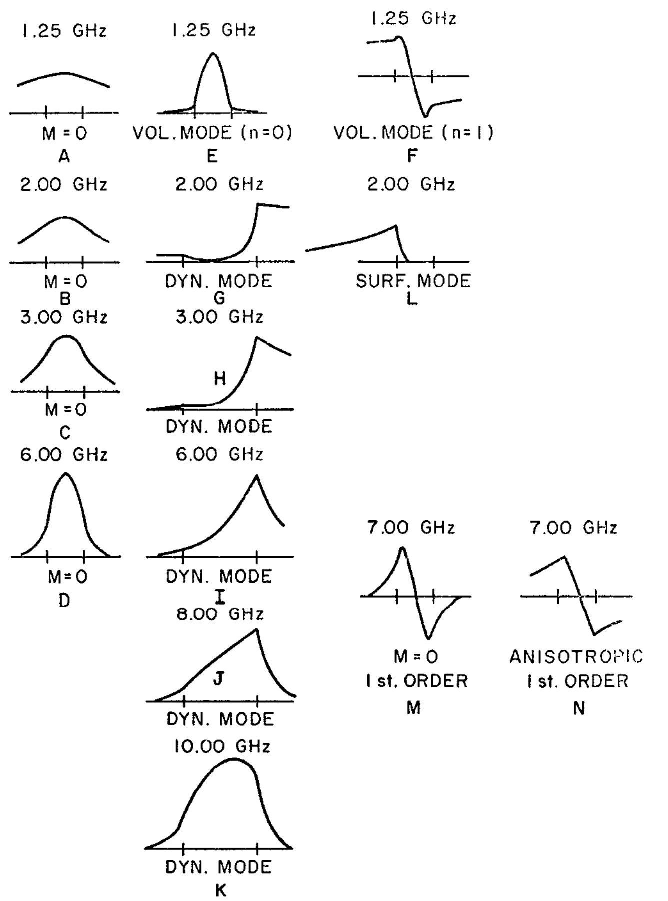

FIGURE 6 ⟶

Transverse Electric Field Distributions for the Dispersion Characteristics of Figure 5.